

# MR Imaging in Patients with Ulnar Collateral Ligament Injury

# 11

Christin A. Tiegs-Heiden, Naveen S. Murthy,  
Brett Lurie, Jan Fritz, and Hollis G. Potter

## Introduction

The ulnar collateral ligament (UCL), also referred to as the medial collateral ligament (MCL) of the elbow, may be injured acutely in the setting of a valgus load to the elbow or as a result of dislocation [1, 2]. In the athlete, the ligament may be chronically stressed by the high valgus loads that are repetitively imparted to the medial side of the elbow during the late cocking phase of throwing. Diagnosing UCL injury in the patient with medial elbow pain can be challenging both clinically and arthroscopically, highlighting the need for accurate diagnostic imaging [3, 4]. MRI offers unparalleled soft-tissue contrast resolution, direct multiplanar imaging capabilities, and high-spatial resolution, allowing for reproducible, accurate, preoperative diagnosis of UCL abnormalities. MRI is also useful postoperatively to assess the integrity of ligament reconstruction and to diagnose potential re-injury.

---

C. A. Tiegs-Heiden · N. S. Murthy (✉)  
Department of Radiology, Mayo Clinic,  
Rochester, MN, USA  
e-mail: [Murthy.naveen@mayo.edu](mailto:Murthy.naveen@mayo.edu)

B. Lurie · J. Fritz · H. G. Potter  
Radiology and Imaging, MRI Division, Hospital  
for Special Surgery, New York, NY, USA

## Technique

MRI of the elbow should be performed at field strengths of 1.5 T or higher, with 3.0 T being preferred. The elbow is typically imaged either in the “superman” position or with the patient in the supine position with the elbow extended at the side and the forearm supinated. Imaging in this position tensions the anterior bundle of the MCL, allowing for more accurate assessment of ligament integrity. If clinically indicated, the posterior bundle of the UCL can be assessed with the elbow in flexion. A phased array surface coil is used to obtain the best possible signal-to-noise ratio [5, 6]. A circumferential coil is necessary to obtain sufficient signal from the posterior elbow structures [7].

The multiplanar capabilities of MRI are extremely valuable for obtaining true sagittal and true coronal images of the obliquely oriented elbow joint [8]. We recommend obtaining three planes of T1 or PD and fluid-sensitive sequences, with a minimum of one T1-weighted sequence. Cartilage and fluid-sensitive pulse sequences are essential for adequate evaluation of all patients. If the elbow is imaged at the patient’s side, inversion recovery sequences are recommended over frequency-selective fat-suppressed sequences due to the magnetic field inhomogeneities encountered away from the isocenter of the bore [7].

High-resolution (512 × 320 matrix, 1.5–2.5 mm slice thickness) intermediate echo time fast spin

echo (FSE) imaging performed in the coronal plane is used to assess the signal intensity of ligaments and tendons as well as regional cartilage status. A high-spatial resolution ( $512 \times 224$  matrix, 1.7-mm slice thickness) small field of view gradient recalled echo (GRE) pulse sequence in the coronal plane yields an in-plane resolution of 300 microns, thus diminishing partial volume and signal averaging, and is useful for assessment of ligament and tendon morphology. Axial and sagittal high-resolution (sagittal  $512 \times 320$  matrix) FSE images with intermediate echo time and slightly increased slice thickness (3.5 mm) are obtained as well to aid in the assessment of the remainder of the elbow structures. Fat-suppressed GRE sequences, which are sensitive to the cartilage of unfused physes, are added for the characterization of growth plates of skeletally immature patients.

Some authors advocate the use of magnetic resonance (MR) arthrography using an intra-articular injection of a gadolinium-based contrast agent or intra-articular saline to aid in the detection of partial tears of the UCL [3, 9]. Distension of the joint capsule with fluid may improve visualization of structures which are normally closely opposed [10]. At the authors' institutions, elbow imaging is performed without the use of intra-articular contrast, preserving MRI as a noninvasive, painless, time efficient, and cost-effective examination. Close attention to high-spatial resolution, noncontrast MRI technique obviates the need for intra-articular contrast [8, 11]. We believe that noncontrast MRI is superior to arthrography for assessment of cartilage, taking advantage of the inherent magnetization transfer contrast provided by intermediate echo time FSE, and that synovitis and patterns of synovial proliferation are better assessed without the confounding factor of a joint distended with contrast material.

---

## Imaging Anatomy

The UCL is a cord-like structure, which averages 27 mm in length and 4–5 mm in width [12]. The

three components of the UCL are the anterior bundle, posterior bundle, and transverse bundle [13]. The anterior bundle is further divided into biomechanically distinct anterior and posterior bands, which are taut at different degrees of flexion and extension and serve as the primary restraint to valgus stress [14–16]. The anterior bundle originates on the undersurface of the medial epicondyle and inserts on the ulna at or within 1–2 mm of the anteromedial facet of the coronoid process, the sublime tubercle [17]. The posterior bundle forms the floor of the cubital tunnel and is more of a thickening of the posterior capsule than a distinct ligament [13]. The transverse bundle runs between the tip of the olecranon and the coronoid process and does not contribute significantly to elbow stability. Neither the posterior nor the transverse bundles are routinely assessed on standard MR imaging with the elbow in extension.

---

## Normal Appearance of the UCL

The UCL is best assessed on coronal images using the GRE and FSE sequences to assess morphology and the STIR and FSE sequences to assess signal intensity.

The intact UCL is thin, vertically oriented, and uniformly low-signal intensity reflecting its composition of highly organized type I collagen (Fig. 11.1; [18]). A normal infolding of synovium may be identified deep to the humeral origin of the posterior band of the anterior bundle, which should not be misinterpreted as a tear [1, 3, 4]. Interdigitation of fat can also be seen at the origin of the posterior band of the anterior bundle, resulting in a slightly striated appearance to the ligament in some patients [17, 19]. The humeral origin of the anterior bundle is fairly broad, with convergence of the ligament as it approaches its insertion on the ulna, where the ligament is continuous with the ulnar periosteum [6, 17, 20]. The deep muscle fibers of the flexor digitorum superficialis are closely apposed to the outer surface of the UCL.



**Fig. 11.1** Coronal intermediate echo time FSE MR image of a normal thin, vertically oriented and hypointense UCL (*white arrow*). Note the normal infolding of synovium and fat deep to the ligament (*black arrow*)



**Fig. 11.2** Coronal FSE MR image demonstrating acute on chronic injury to the UCL. The *long black arrow* indicates a complete tear of the thickened posterior band of the anterior bundle. Adjacent soft-tissue edema is noted within the flexor pronator muscles (*short arrow*)

## MR Findings in UCL Injury

### Acute Injury

Acute injuries to the UCL are seen as areas of altered signal intensity, altered morphology, or indistinctness of the normally hypointense, vertically oriented ligament [1, 4]. There may be a discontinuity of some or all of the fibers of the UCL with or without retraction (Fig. 11.2; [6]). Adjacent soft-tissue edema as well as injury to the flexor pronator origin may serve as additional evidence of an acute injury (Fig. 11.3).

Tears of the UCL are most commonly at the humeral origin of the ligament, while midsubstance and distal tears are less common (Fig. 11.4; [5]). Avulsion fractures of the sublime tubercle or of traction osteophytes may also be seen (Fig. 11.5; [11]).

Partial thickness tears of the UCL are further classified as high-grade partial or low-grade par-

tial, which are differentiated based on the involvement of more or less than 50% of the ligament thickness, respectively (Fig. 11.6; [21]). A focal defect in the ligament may be seen, but more commonly, partial thickness tears are diagnosed on the basis of ligament indistinctness and hyperintensity. Fluid imbibition can help to delineate an acute tear, but the absence of this sign does not exclude injury to the ligament (Fig. 11.7).

The “T-sign” describes the appearance of fluid extending distally between the ulna and the UCL due to stripping of deep fibers of the ligament off the sublime tubercle (Fig. 11.8; [3]). While originally described with computed tomography (CT) and MR arthrography, a T-sign can be observed in nonarthrographic MRI provided that close attention is paid to MR technique. It is commonly held that nonarthrographic MRI has a relatively low sensitivity for the detection of partial thickness tears, somewhere in the order of 57% [3]. The use of high-resolution, fluid-sensitive inter-



**Fig. 11.3** Coronal FSE image shows an acute complete tear of the flexor pronator origin (*long black arrow*) with retraction (*short black arrow*). The UCL ligament appears high signal and slightly ill-defined reflecting concomitant low-grade injury to the UCL (*white arrow*)



**Fig. 11.4** Coronal FSE MR image shows a complete tear of the anterior band of the anterior bundle of the UCL off its ulnar insertion (*arrow*)

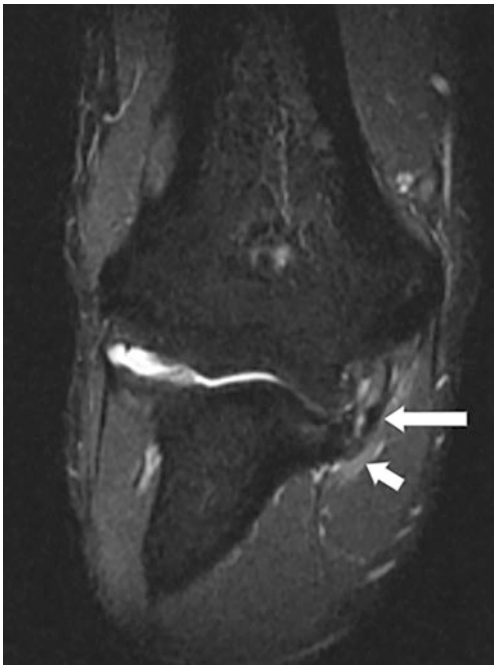


**Fig. 11.5** Coronal STIR image shows an avulsion fracture of an osteophyte arising off the ulna (*long arrow*). Adjacent soft-tissue edema is indicated by the *short arrow*



**Fig. 11.6** Coronal FSE MR image demonstrating intra-substance high signal (*arrow*) indicative of a low-grade interstitial partial tear at the humeral origin of the posterior band of the anterior bundle of the UCL



**Fig. 11.7** Coronal STIR image shows a high-grade partial tear of the posterior band of the anterior bundle of the UCL (*long arrow*). A reactive marrow edema pattern is seen within the medial epicondyle reflecting a stress reaction (*short arrow*)



**Fig. 11.8** Coronal STIR MR image shows fluid between the UCL and the sublime tubercle (*T-sign*) indicating avulsion of deep fibers of the UCL off the ulna in the setting of an undersurface partial tear (*long arrow*). The *short arrow* shows edema at the humeral origin of the chronically thickened UCL

mediate echo time FSE sequences allows for the diagnosis of partial tears with much higher sensitivity than is typically quoted in the literature for nonarthrographic studies [6, 11].

The term interstitial load can be applied to ligaments that appear stretched, mildly attenuated, and diffusely hyperintense reflecting the presence of interstitial microtears caused by an acute distracting force, without a well-defined partial thickness tear (Fig. 11.9).

MRI-based classification systems for UCL injuries have been proposed. A 6-stage classification system was described by Ramkumar et al. based on the location (proximal, midsubstance, or distal) and degree of tear (partial or complete) [22]. This system demonstrated very good reliability and may aid in decision-making as complete and distal tears are more likely to require operative management [22, 23].

## Chronic Injury

Ligaments subject to chronic repetitive stress may remodel resulting in asymmetric ligament thickening and altered signal intensity, even in the asymptomatic patient (Fig. 11.10; [5, 24]). The chronically stressed UCL may demonstrate plastic deformation appearing lax, redundant, or indistinct [8, 12]. Associated mild ligament hyperintensity has been attributed to the presence of chronic microtears leading to intraligamentous hemorrhage and edema [25]. Foci of intraligamentous calcification or heterotopic ossification may also be identified in the chronically overloaded and repetitively injured UCL (Fig. 11.11).

Osseous stress reactions are also commonly seen and may manifest as a focal bone marrow edema pattern, either at the humerus or at the coronoid process. Chronic valgus stress may also



**Fig. 11.9** Coronal STIR MR image demonstrates diffuse hyperintensity of the posterior band of the anterior bundle of the UCL without focal discontinuity (*short arrow*) indicating the effects of an acute interstitial load. A focal bone marrow edema pattern is seen at the ulna reflecting a mild stress reaction (*long arrow*)

result in osseous remodeling on the medial side of the elbow resulting in traction osteophytes, which may be subject to fracture or avulsion in the setting of acute on chronic injury.

### Associated Elbow Findings in Chronic Valgus Overload

Chronic valgus overload to the elbow results in attritional attenuation of the UCL leading to laxity and eventual ligament failure [25]. Prior to ligament failure, the chronically stressed elbow will develop osteoarthritic changes as a result of excessive posteromedial joint contact. Subchondral sclerosis may be observed over the posteromedial aspect of the ulna and the corresponding posterior aspect of the trochlea, reflecting the presence of subchondral bony remodeling (Fig. 11.12). Another early sign of posteromedial impingement is prominent synovitis within the

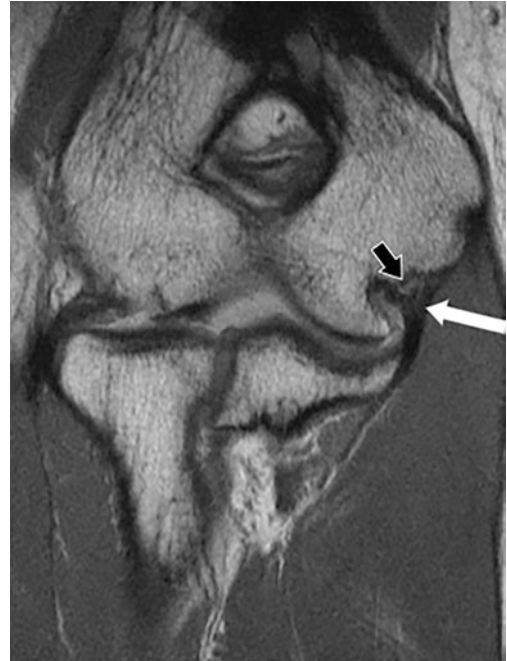


**Fig. 11.10** Coronal FSE MR image of a chronically remodeled UCL ligament in a pitcher (*white arrow*). The ligament is thicker than usual but is still uniformly hypointense. A small traction spur is noted arising off the slightly bulbous medial epicondyle (*black arrow*)



**Fig. 11.11** Coronal FSE MR image demonstrates a focus of intraligamentous ossification in a chronically injured UCL (*arrow*)

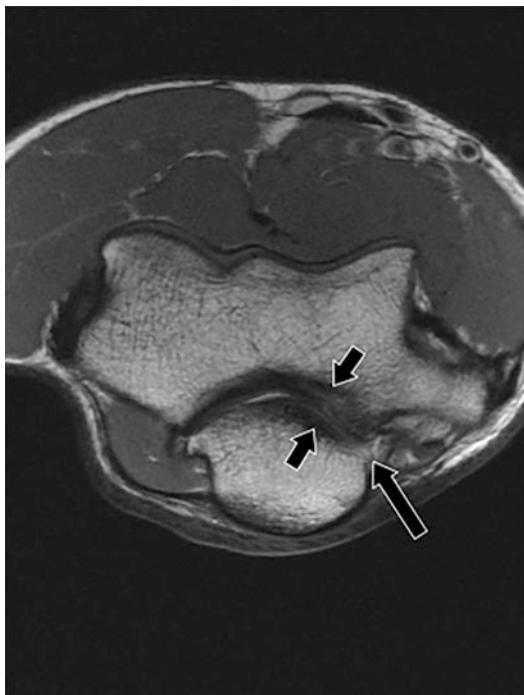


**Fig. 11.12** Axial FSE MR image demonstrating features of posteromedial impingement in the setting of chronic valgus extension overload. The *short arrows* indicate subchondral sclerosis, chronic bony remodeling, and partial cartilage wear in the posteromedial humeroulnar compartment. The *long arrow* shows a developing osteophyte off the medial aspect of the olecranon process

posteromedial joint capsule, which is most easily appreciated on sagittal and axial FSE images (Fig. 11.13). As posteromedial impingement continues, chondral thinning may be observed at the posteromedial ulnohumeral articulation, leading to the development of osteophytes usually on the olecranon [24]. In chronic posteromedial impingement, there may also be intra-articular loose bodies due to chondral injury. Fractured osteophytes are also commonly seen and can be visualized on the far posterior images of the coronal series or on axial images. A lateral radiograph in maximum flexion is also efficacious in defining the osteophytes. The inability to obtain full extension of the elbow should prompt a search for additional evidence of posteromedial impingement.

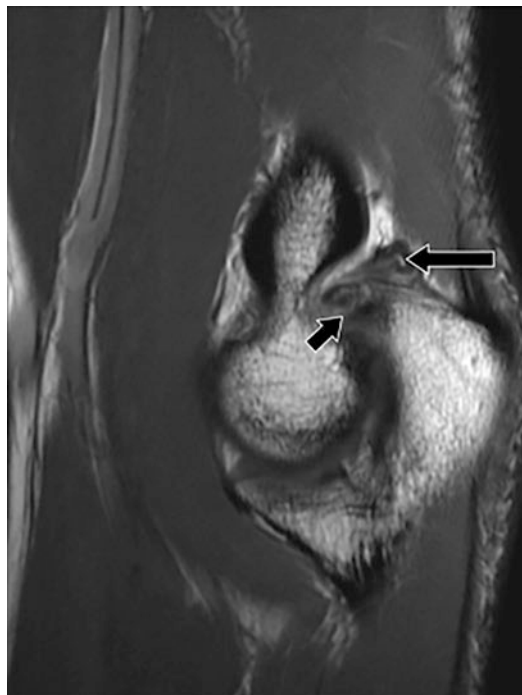


**Fig. 11.13** Sagittal FSE MR image shows additional findings of posteromedial impingement with marked synovial scarring at the posteromedial aspect of the elbow joint surrounding a loose body (*long arrow*). The *short arrow* indicates a chronic fracture through an olecranon osteophyte

## Flexor Tendinopathy and Tears

An acute valgus load to the elbow is frequently accompanied by contusion or tears of the flexor pronator origin with extensive soft-tissue edema [2]. Excessive tension on the medial elbow soft tissues in the setting of chronic valgus extension overload may also lead to the development of tendinosis and tears, most commonly affecting the pronator teres and the flexor carpi radialis [1]. Tendinosis manifests on MRI as intermediate to increased T2 signal intensity within the tendon, often with focal enlargement (Fig. 11.14). The observed areas of increased signal intensity correspond to areas of collagen disruption, mucoid or hyaline degeneration, and neovascularization [26]. Areas of heterotopic ossification or dystro-

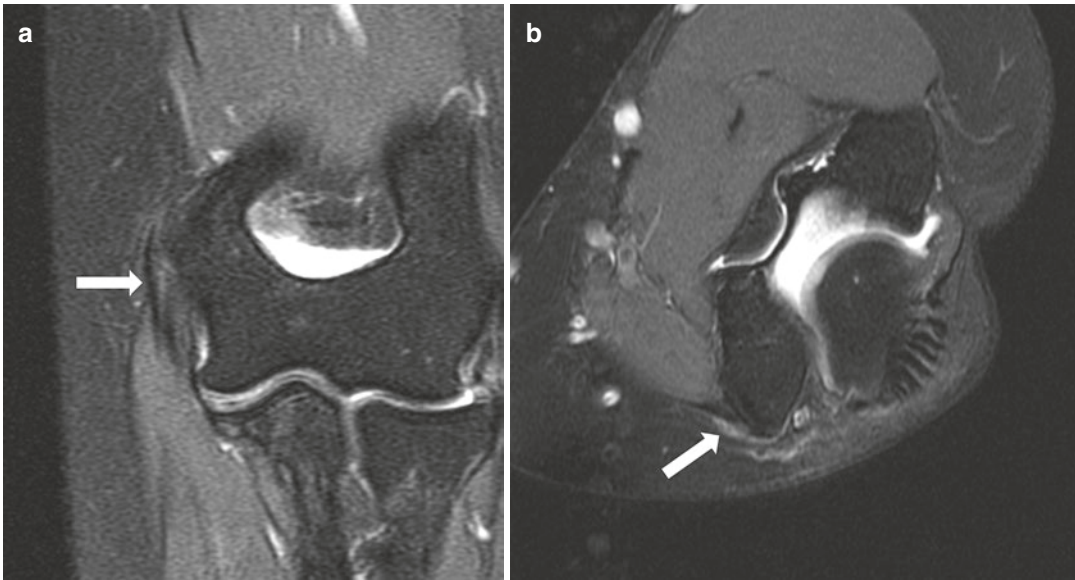


**Fig. 11.14** Coronal (a) and axial (b) T2 FSE MR images with fat saturation demonstrating mild increased signal and focal enlargement of the flexor carpi radialis origin compatible with mild tendinopathy (*arrows*)

phic calcification may also be observed at the origin of previously injured or chronically degenerated tendons.

### Ulnar Neuropathy

Ulnar neuritis may manifest on MRI as nerve or fascicular enlargement within or more typically proximal to the cubital tunnel. The normal fascicular architecture of the nerve can be disrupted, and the nerve may appear hyperintense on both FSE and inversion recovery pulse sequences (Fig. 11.15). Masses, osteophytes, ganglia, and accessory muscles may all cause impingement of the ulnar nerve in the cubital tunnel [27], but in the throwing athlete, ulnar neuritis is more frequently a result of chronic traction caused by excessive valgus laxity. Morphological and signal alterations within the ulnar nerve are a frequent finding even in the asymptomatic patient, highlighting the importance of interpreting the MR findings in the context of clinical symptoms.

### Radiocapitellar Osteochondral Defects

Injury to the cartilage of the radiocapitellar compartment can occur in the setting of an acute valgus load or following dislocation due to direct impaction of the radius against the capitellum. Capitellar osteochondral lesions may also develop in the context of valgus extension overload (Fig. 11.16). The possibility of associated osteochondral lesions in the setting of acute and chronic UCL injury underscores the importance of cartilage-sensitive imaging in all patients, as these lesions reflect a primary ischemic insult to subchondral bone and the overlying cartilage represents the “innocent bystander” of the process [8]. Mild chondral hyperintensity and subchondral flattening may serve as early evidence of an osteochondral lesion, formerly termed osteochondritis dissecans [28]. As changes progress, there may be frank subchondral collapse, cystic resorption of subchondral bone, fluid imbibition between the osteochondral lesion and the parent bone, or a loose osteochondral fragment.

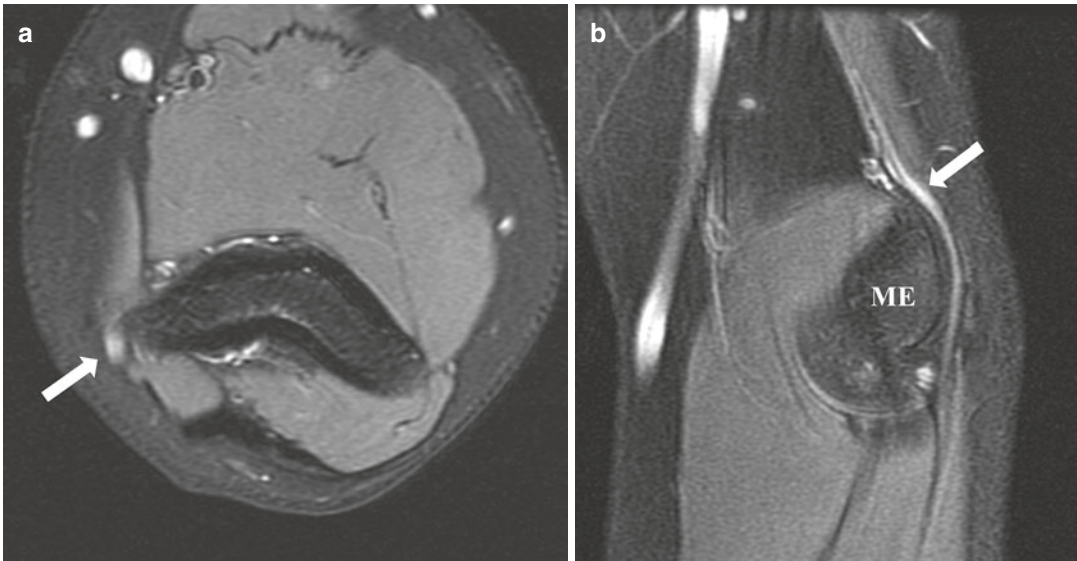


**Fig. 11.15** Overhead throwing athlete with recalcitrant ulnar neuropathy despite conservative management. Axial (a) and sagittal (b) T2 FSE MR images with fat saturation

showing mild increased signal and enlargement of the ulnar nerve just proximal to the cubital tunnel (*arrows*). ME, medial humeral epicondyle

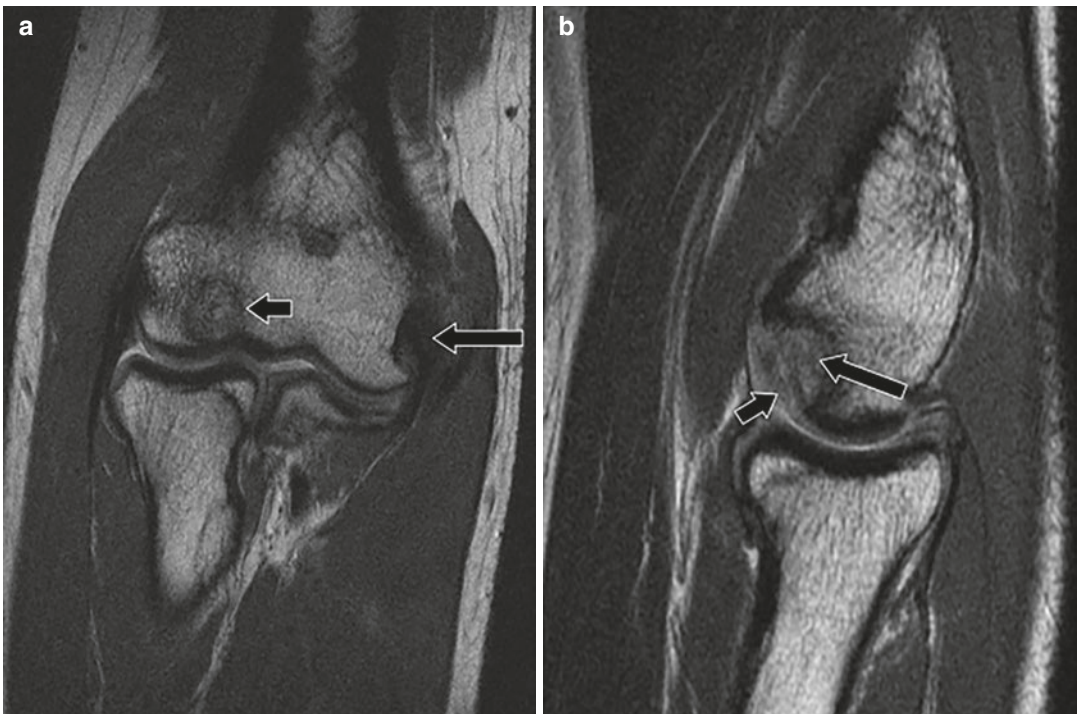


**Fig. 11.16** (a) Coronal FSE image demonstrates chronic thickening of the UCL in a throwing athlete (*long arrow*). The *short arrow* indicates a capitellar osteochondral lesion. (b) Sagittal FSE image in the same patient demonstrates a

capitellar osteochondral lesion (*long arrow*) with loss of the tidemark, subchondral collapse, cystic resorption of subchondral bone, and early fragmentation. The overlying cartilage (*short arrow*) is markedly hyperintense

## Apophyseal Injury

In the skeletally immature athlete, acute and chronic stresses to the UCL are preferentially transmitted to the medial epicondylar apophysis with relatively little observable change in the ligament itself [29]. A Salter Harris I fracture may occur with variable degrees of separation of the medial epicondylar apophysis (Fig. 11.17). Associated bone marrow edema patterns may be present in the apophysis. In the chronic setting, a traction apophysitis may be seen with widening of the growth plate or fragmentation of the epicondylar apophysis [5]. The observation of a bulbous contour to the medial epicondyle may serve as evidence of remote apophyseal injury prior to physal fusion.



**Fig. 11.17** Coronal GRE image demonstrating chronic widening of the unfused medial epicondylar apophysis in a skeletally immature pitcher (*long arrow*). The UCL ligament (*short arrow*) is mildly thickened but otherwise unremarkable in appearance reflecting the preferential transmission of valgus force to the apophysis

## Postsurgical Elbow

UCL reconstruction is the primary procedure available to restore medial elbow stability and relieve elbow pain in patients with injury to the UCL [30]. MRI following ligament reconstruction is technically challenging due to the presence of metallic debris and associated susceptibility artifact (Fig. 11.18). This is particularly prominent on gradient recalled sequences due to the lack of a 180° rephasing pulse, limiting the utility of this sequence in the postoperative setting [6]. Interpreting the postoperative MRI is also diagnostically challenging due to the wide spectrum of “normal” postoperative appearances and varying approaches to ligament reconstruction.

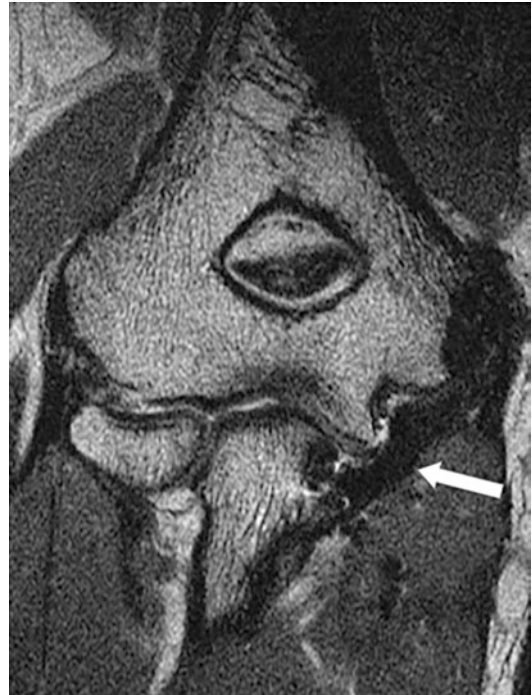


**Fig. 11.18** Coronal FSE image in a patient following UCL ligament reconstruction. The *white arrow* indicates a normal appearing graft, which is thicker than the native ligament but demonstrates uniform hypointensity and appears taut in extension. Note the small foci of magnetic susceptibility adjacent to the sublime tubercle

MRI in the postoperative elbow is useful for the assessment of the integrity of the reconstruction, detecting stress fractures, for the visualization of the transposed and nontransposed ulnar nerve, for the assessment of cartilage integrity, and for the evaluation of the remainder of the elbow and adjacent soft tissues (Fig. 11.19; [31]).

The reconstructed UCL is much thicker than the native UCL reflecting the double bundle nature of most grafts and the remnant native UCL. The well-functioning graft should appear taut in extension [31]; graft dysfunction may be suspected when the graft appears lax or redundant. Graft signal intensity is more difficult to interpret as the signal may vary depending on the

time since surgery and the degree of remodeling. Heterotopic ossification may be seen within and adjacent to a reconstructed UCL, rarely resulting in bony bridging or fibrous bridging at the humerus or the ulna (Fig. 11.20a). A partial or complete re-tear of the graft can be confidently diagnosed when there is linear fluid imbibition into a focal discontinuity of the graft (Fig. 11.20b). Interstitial partial tearing may also be seen as redundancy or outward bowing of the graft or new high signal within a graft [32]. On the rare occasion when heterotopic ossification is extensive, a re-tear may be identified as a fracture through a fibrous union between the ossified ligament and the humerus or ulna.

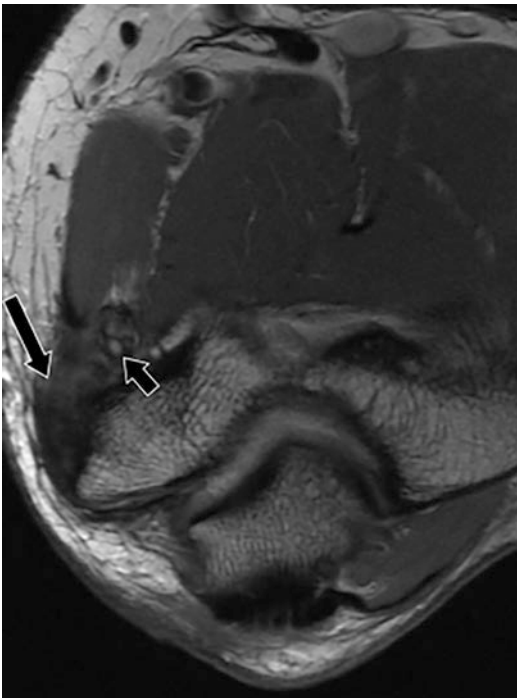


**Fig. 11.19** Axial FSE image in patient following repair of the flexor pronator origin (*long arrow*) shows a transposed ulnar nerve which is encased in hypertrophic scar (*short arrow*). The nerve is hyperintense with marked enlargement of individual nerve fascicles reflecting ulnar neuritis



**Fig. 11.20** (a) AP radiograph demonstrates multiple foci of heterotopic ossification within a reconstructed UCL (*arrow*). (b) Corresponding FSE MRI demonstrates the appearance of heterotopic ossification on MRI (*short arrow*). A near complete tear of the reconstruction is indicated by fluid imbibition into a defect in the partially ossified ligament (*long arrow*)

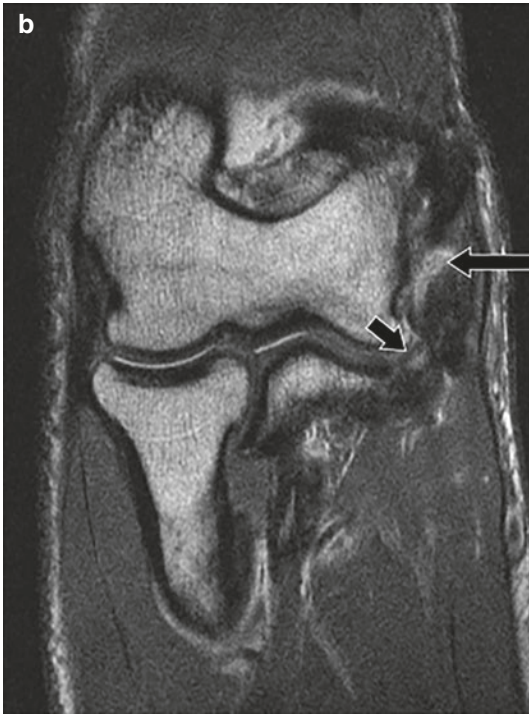


**Fig. 11.20** (continued)

## Conclusion

MR imaging of the elbow allows for accurate and early diagnosis of acute, chronic, and acute on chronic injuries to the UCL. Optimized high-spatial resolution and high soft-tissue contrast MR imaging may reveal several abnormalities that could potentially contribute to elbow pain and dysfunction, particularly in the throwing athlete. The importance of a thorough history, clinical examination, and a good working relationship between the interpreting radiologist and the referring clinician cannot be overstated.

## References

1. Kijowski R, Tuite M, Sanford M. Magnetic resonance imaging of the elbow. Part II: abnormalities of the ligaments, tendons, and nerves. *Skeletal Radiol.* 2004;34(1):1–18.
2. Richard MJ. Traumatic valgus instability of the elbow: pathoanatomy and results of direct repair. *J Bone Joint Surg Am.* 2008;90(11):2416.

3. Timmerman LAL, Schwartz MLM, Andrews JRJ. Preoperative evaluation of the ulnar collateral ligament by magnetic resonance imaging and computed tomography arthrography. Evaluation in 25 baseball players with surgical confirmation. *Am J Sports Med.* 1994;22(1):26–32.
4. Gaary EA, Potter HG, Altchek DW. Medial elbow pain in the throwing athlete: MR imaging evaluation. *AJR Am J Roentgenol.* 1997;168(3):795–800. (PubMed—NCBI).
5. Potter HG, Ho ST, Altchek DW. Magnetic resonance imaging of the elbow. *Semin Musculoskelet Radiol.* 2004;8(1):5–16. (Copyright© 2004 by Thieme Medical Publishers, Inc., 333 Seventh Avenue, New York, NY 10001, USA).
6. Kaplan LJ, Potter HG. MR imaging of ligament injuries to the elbow. *Radiol Clin N Am.* 2006;44(4):583–94.
7. Johnson D, Stevens KJ, Riley G, Shapiro L, Yoshioka H, Gold GE. Approach to MR imaging of the elbow and wrist: technical aspects and innovation. *Magn Reson Imaging Clin N Am.* 2015;23(3):355–66.
8. Potter HG. Imaging of posttraumatic and soft tissue dysfunction of the elbow. *Clin Orthop Relat Res.* 2000;(370):9–18.
9. Magee T. Accuracy of 3-T MR arthrography versus conventional 3-T MRI of elbow tendons and ligaments compared with surgery. *AJR Am J Roentgenol.* 2015;204(1):W70–5.
10. LiMarzi GM, O'Dell MC, Scherer K, Pettis C, Wasyliw CW, Bancroft LW. Magnetic resonance arthrography of the wrist and elbow. *Magn Reson Imaging Clin N Am.* 2015;23(3):441–55.
11. Salvo JP, Rizio L, Zvijac JE, Uribe JW, Hechtman KS. Avulsion fracture of the ulnar sublime tubercle in overhead throwing athletes. *Am J Sports Med.* 2002;30(3):426–31.
12. Mirowitz SAS, London SLS. Ulnar collateral ligament injury in baseball pitchers: MR imaging evaluation. *Radiology.* 1992;185(2):573–6.
13. Bryce CDC, Armstrong ADA. Anatomy and biomechanics of the elbow. *Orthop Clin North Am.* 2008;39(2):141–54.
14. Hotchkiss RN, Weiland AJ. Valgus stability of the elbow. *J Orthop Res.* 1987;5(3):372–7.
15. Callaway GH, Field LD, Deng XH, Torzilli PA, O'Brien SJ, Altchek DW, et al. Biomechanical evaluation of the medial collateral ligament of the elbow. *J Bone Joint Surg Am.* 1997;79(8):1223–31.
16. Morrey BF, An K. Functional anatomy of the ligaments of the elbow. *Clin Orthop Relat Res.* 1985;201:84–90.
17. Munshi M, Pretterklieber ML, Chung CB, Haghighi P, Cho JH, Trudell DJ, et al. Anterior bundle of ulnar collateral ligament: evaluation of anatomic relationships by using MR imaging, MR arthrography, and gross anatomic and histologic analysis. *Radiology.* 2004;231(3):797–803.
18. Gustas CN, Lee KS. Multimodality imaging of the painful elbow: current imaging concepts and image-

- guided treatments for the injured Thrower's elbow. *Radiol Clin N Am.* 2016;54(5):817–39.
19. Husarik DB, Saupé N, Pfirrmann CWA, Jost B, Hodler J, Zanetti M. Ligaments and plicae of the elbow: normal MR imaging variability in 60 asymptomatic subjects. *Radiology.* 2010;257(1):185–94.
  20. Sugimoto H, Ohsawa T. Ulnar collateral ligament in the growing elbow: MR imaging of normal development and throwing injuries. *Radiology.* 1994;192(2):417–22.
  21. Kim NR, Moon SG, Ko SM, Moon W-J, Choi JW, Park J-Y. MR imaging of ulnar collateral ligament injury in baseball players: value for predicting rehabilitation outcome. *Eur J Radiol.* 2011;80(3):e422–6.
  22. Ramkumar PN, Frangiamore SJ, Navarro SM, Lynch TS, Forney MC, Kaar SG, et al. Interobserver and intraobserver reliability of an MRI-based classification system for injuries to the ulnar collateral ligament. *Am J Sports Med.* 2018;46(11):2755–60.
  23. Ramkumar PN, Haeberle HS, Navarro SM, Frangiamore SJ, Farrow LD, Schickendantz MS. Prognostic utility of an magnetic resonance imaging-based classification for operative versus nonoperative management of ulnar collateral ligament tears: one-year follow-up. *J Shoulder Elb Surg.* 2019;28(6):1159–65.
  24. Hurd WJ, Eby S, Kaufman KR, Murthy NS. Magnetic resonance imaging of the throwing elbow in the uninjured, high school-aged baseball pitcher. *Am J Sports Med.* 2011;39(4):722–8.
  25. Dodson CC, Thomas A, Dines JS, Nho SJ, Williams RJ, Altchek DW. Medial ulnar collateral ligament reconstruction of the elbow in throwing athletes. *Am J Sports Med.* 2006;34(12):1926–32.
  26. Potter HGH, Hannafin JAJ, Morwessel RMR, DiCarlo EFE, O'Brien SJS, Altchek DWD. Lateral epicondylitis: correlation of MR imaging, surgical, and histopathologic findings. *Radiology.* 1995;196(1):43–6.
  27. Hash T, Bogner E. Nerve entrapment and compression syndromes of the elbow. *Semin Musculoskelet Radiol.* 2010;14(4):438–48.
  28. Sofka CM, Potter HG. Imaging of elbow injuries in the child and adult athlete. *Radiol Clin N Am.* 2002;40(2):251–65.
  29. Benjamin HJH, Briner WW Jr. Little league elbow. *Clin J Sport Med.* 2005;15(1):37–40.
  30. Jobe FWF, Stark HH, Lombardo SJS. Reconstruction of the ulnar collateral ligament in athletes. *J Bone Joint Surg Am.* 1986;68(8):1158–63.
  31. Wear SA, Thornton DD, Schwartz ML, Weissmann RC III, Cain EL, Andrews JR. MRI of the reconstructed ulnar collateral ligament. *Am J Roentgenol.* 2011;197(5):1198–204.
  32. Daniels SP, Mintz DN, Endo Y, Dines JS, Sneag DB. Imaging of the post-operative medial elbow in the overhead thrower: common and abnormal findings after ulnar collateral ligament reconstruction and ulnar nerve transposition. *Skelet Radiol.* 2019;48:1843–60.